Geophysical evidence that Saturn's Moon Phoebe originated from a C-type asteroid reservoir

Julie Castillo-Rogez, Pierre Vernazza, Kevin Walsh

Monthly Notices
of the
ROYAL ASTRONOMICAL SOCIETY

MNRAS **486,** 538–543 (2019)
Advance Access publication 2019 March 19

doi:10.1093/mnras/stz786

Geophysical evidence that Saturn's Moon Phoebe originated from a C-type asteroid reservoir

Julie Castillo-Rogez [1]★ Pierre Vernazza[2] and Kevin Walsh[3]

[1] *Jet Propulsion Laboratory, California Institute of Technology, Pasadena, CA 91109, USA*
[2] *Laboratoire d'Astrophysique de Marseille, UMR 7326 LAM, 13007 Aix-Marseille Universite, France*
[3] *Southwest Research Institute, Boulder, CO 80309, USA*

Accepted 2019 February 28. Received 2019 February 22; in original form 2018 December 14

ABSTRACT

Saturn's Moon Phoebe has been suggested to originate from the Kuiper Belt. However, its density is twice that of Kuiper Belt objects (KBOs) in the same size class, which challenges that relationship. Since the internal evolution of mid-sized planetesimals (100–300 km in diameter) is primarily driven by the amount of accreted short-lived radioisotopes, it is possible to constrain the relative times of formation of these bodies based on their bulk porosity content, hence their densities. From modelling the thermal evolution of KBOs, we infer a difference in formation timing between these bodies and Phoebe. This confirms prior suggestions for a delayed accretion timeframe with increasing distance from the Sun. This geophysical finding combined with spectral observations suggests Phoebe formed in the same region as C-type asteroids and support recent dynamical models for a C-type body reservoir between the orbits of the giant planets. On the other hand, the similarly low densities of mid-sized D-type asteroids, Trojan asteroids, and KBOs add to the growing evidence that these objects shared a common reservoir near or beyond the orbit of Neptune and were heat starved overall.

Key words: Kuiper belt: general – minor planets, asteroids: general – planets and satellites: interiors.

1 INTRODUCTION

The main belt of asteroids is composed of a variety of bodies. About half of the mass of the main belt is encompassed in the four most massive asteroids (Ceres, Vesta, Pallas, Hygiea). The rest of the main belt mass is dominated by mid-sized (100–300 km diameter) asteroids, which are believed to be the source of the many fragments found in the belt (Bottke et al. 2005; Cuzzi, Hogan & Bottke 2010) and the progenitors of asteroid families (Dermott et al. 2018). The current status quo is that these planetesimals accreted fast (Morbidelli et al. 2009) and thus represent the first generation of large bodies in the Solar system (Bottke et al. 2005; Cuzzi et al. 2010). That class of bodies is a common feature of all the reservoirs of small bodies, although these objects are most frequently found in the main belt of asteroids and the Kuiper Belt. They are scarcer among the Jupiter Trojan asteroid clusters and irregular satellites (Fig. 1).

In water-rich mid-sized bodies, long-lived radioisotopes, which deliver their heat over billion-year time-scales, have little bearing on internal evolution, especially since ice thermal conductivity is very high (5–16 W m^{-1} K^{-1}, Andersson & Inaba 2005) at the temperatures of interest. Furthermore, in their detailed review of small body heat sources, Leliwa-Kopystynski & Kossacki (2000) showed that accretional energy is a marginal heat source in bodies less than 500 km diameter. Hence, this leaves short-lived radioisotopes as the primary driver of thermal evolution in these objects. Their impact is a function of the relative fractions of rock and ice. The role of short-lived radioisotopes, and especially aluminum-26 (^{26}Al), in driving aqueous alteration in the parent bodies of carbonaceous chondrites was recognized early on (e.g. Schramm, Tera & Wasserburg 1970). In particular, the class of C*h* asteroids, most within 100–300 km, show evidence for aqueous alteration (Rivkin et al. 2015) and are believed to be parent bodies of the CM chondrites (e.g. Young et al. 1999; Young, Zhang & Schubert 2003; McAdam et al. 2015; Vernazza et al. 2016). Short-lived radioisotopes are also believed to have played a major role in the evolution of mid-sized Kuiper Belt objects (KBOs) and other transneptunian objects (TNOs) (e.g. Prialnik et al. 2008; Shchuko et al. 2014). However, the density data returned for representatives of these reservoirs over the past decade instead suggest they have preserved a large fraction of porosity, which is evidence for weakly evolved objects. On the other hand, Saturn's moon Phoebe, which was suggested to come from the Kuiper Belt (e.g. Johnson & Lunine 2005), has a density that is almost twice that of observed at KBOs.

We summarize the state of knowledge of 100–300 km planetesimals in Section 2. We use porosity as a gauge of internal evolution, following the approach of Castillo-Rogez et al. (2017), to compare the internal states of bodies formed with different

★ E-mail: Julie.C.Castillo@jpl.nasa.gov

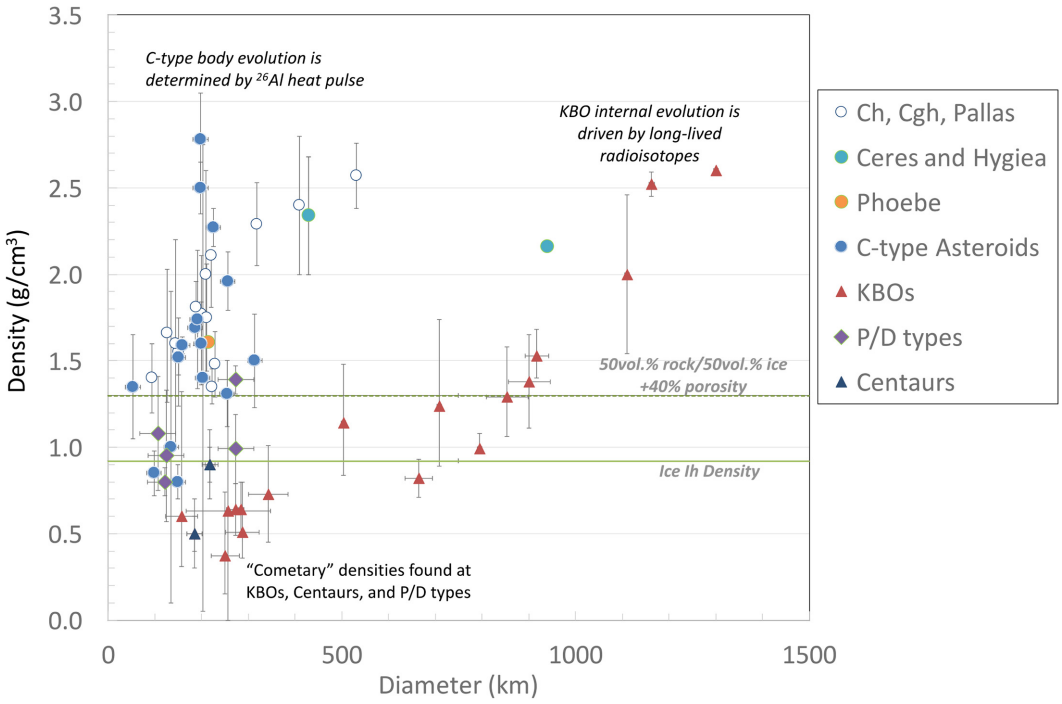

Figure 1. Bulk densities of minor planets less than 1500 km in diameter. Ice I density (solid line) and a mixture of 50 vol. per cent rock/50 vol. per cent ice with 40 per cent porosity added (dashed line) are shown for reference. The spread in the 100–300 km region illustrates the contrast in remnant porosity and thus heat budget available to these various classes of bodies. Two clusters of bodies can be distinguished with densities $<\sim$1 g cm^{-3} and $>\sim$1.3 g cm^{-3}. Additional data for large (>1000 km) KBOs is provided to support the discussion. References for asteroids: Yeomans et al. (1997); Müeller et al. (2009); Somenzi et al. (2011) ; Marchis et al. (2006, 2008, 2012, 2013); Baer & Chesley (2008); Baer et al. (2011); Goffin (2014); Hanuš et al. (2017a,b); Pajuelo et al. (2018). References for TNOs: Meech et al. (1997); Tegler et al. (2005); Grundy et al. (2012); Vilenius et al. (2012); Brown (2013); Marchis et al. (2014).

amounts of (live) ^{26}Al. We focus on the modelling of KBO internal evolution for comparison with the Castillo-Rogez et al. (2012) modelling of Phoebe, as presented in Section 3. Since ^{26}Al has a short half-life ($\sim$0.71 My), the amount of ^{26}Al required to explain observed densities can been used as a chronometer, i.e. to constrain the time at which bodies fully assembled. Hence, our results lead to new constraints on the relative formation timing of small bodies reservoirs found across the Solar system and their genetic relationships, as discussed in Section 4.

2 OVERVIEW OF PLANETESIMAL DENSITIES

Hydrated C-type asteroids (C*h* and C*gh*-types) have densities in the 1.4–2.5 g cm^{-3} range (e.g. Hanuš et al. 2017) with a marked dependence on size, as previously noted by Carry (2012). That density range may reflect a low fraction of free volatiles (ice) combined with a low porosity fraction, especially at increasing sizes. Densities between 1.6 and 2.2 g cm^{-3} obtained for bodies 100–200 km in diameter matches their meteoritic analogues, namely CM chondrites (average density $\sim$2.1 g cm^{-3}, Consolmagno, Britt & Macke 2008). Times of formation for these bodies believed to be parent bodies of CM chondrites (Vernazza et al. 2016) is 3.5 My after CAIs (Jogo et al. 2017) assuming a canonical ^{26}Al/^{27}Al $= 5.5 \times 10^{-5}$. Densities of IDP-like C-type asteroids (these objects represent $\sim$50 per cent of C-complex asteroids and possess spectral properties unlike those of CM chondrites; Vernazza et al. 2015, 2017) show a large spread, beyond the large uncertainties, with densities ranging between 1.0–1.6 g cm^{-3} for bodies in the 100–200 km size range.

Many irregular satellites share several similarities with C-asteroids. This is the case of Saturn's irregular satellite Phoebe, high-density body (1.67 g cm^{-3}, Thomas et al. 2007). Outer Solar system bodies in the same size range for which density data are available (besides icy moons) show much lower densities (Fig. 1). Phoebe also displays expressions of aqueous alteration and geophysical evolution explained by an early phase of melting driven by ^{26}Al decay heat (Castillo-Rogez et al. 2012) and an ice-rich subsurface (below the regolith) (Clark et al. 2005; Fraser & Brown 2018). The density of another irregular satellite, Jupiter's moon Himalia was inferred to be also about 1.63 g cm^{-3}, assuming a mean radius of $\sim$85 km (Cruikshank 1977), and even larger for the lower bound on radius determination of $\sim$65 km (Porco et al. 2003). Detailed analysis of Himalia's impact on the orbits of neighbouring satellites by Brozovic & Jacobson (2017) yields a similar density, between 1.55 and 2.26 g cm^{-3}.

On the other hand, KBOs smaller than 500 km in diameter have densities around 0.6 g cm^{-3} and down to 0.3 g cm^{-3}, whereas those objects bigger than 800 km have densities >1 g cm^{-3} (Stansberry et al. 2012; Brown 2013). Above 500 km diameter, KBOs show a quasi-linear density dependence on size, up to 2.5 g cm^{-3} (Brown 2013). Brown (2013) pointed out that the density of 0.82 ± 0.11 g cm^{-3} he inferred for the 650-km large 2002UX25 reflects both substantial porosity and a deficit in rock. Larger KBOs have densities that do reflect a rock-rich interior. This diversity has been interpreted by Barr & Schwamb (2016) as evidence for the partial removal of ice shells from differentiated KBOs. Hence, rock scarcity cannot uniquely account for the large porosity preserved in mid-sized KBOs.

P- and D-type asteroids found in the main belt have relatively low densities: $\sim$1 g cm^{-3} for the large (250 km) 65 Cybele and its family members: e.g. 87 Sylvia (1.2 $\pm$ 0.15 g cm^{-3}, Marchis et al. 2012). Furthermore, large D- and P-types do not show evidence for hydration, similarly to Trojan asteroids. The $\sim$270 km P-type 65 Cybele's surface displays water ice (Licandro et al. 2011). Few density measurements have been obtained for Trojan asteroids: $0.8^{+0.2/-0.1}$ g cm^{-3} for Patroclus (Marchis et al. 2006) and 1 $\pm$ 0.2 g cm^{-3} for Hektor (Marchis et al. 2014), although a much higher estimate of 2.43 $\pm$ 0.35 g cm^{-3} has been suggested for the latter (Descamps 2015). Marchis et al. (2014) pointed out that the difference between the densities of Patroclus and Hektor is consistent with the difference in compaction driven by the pressures that can be reached in these objects, assuming that they started with similar, volatile-rich compositions.

Density measurements are lacking for Centaurs, but indirect observations also suggest these objects have low densities. For example, an upper bound density of 0.9 g cm^{-3} was derived for the $\sim$200-km large Chiron (Meech et al. 1997) and the $\sim$190 km Pholus has a density of the order of 0.5 g cm^{-3} (Tegler et al. 2005). A large TNOs, the 920-km large Orcus has a density of $1.53^{+0.15/-0.13}$ g cm^{-3} (Fornasier et al. 2014). It displays potential spectral evidence for ammonium (Delsanti et al. 2010), a marker of aqueous alteration like in the case of Ceres (De Sanctis et al. 2015), although other types of nitrogen compounds can explain the Orcus spectra (e.g. NH_3, Delsanti et al. 2010).

These discrepancies show that mid-sized planetesimals across the Solar system underwent different evolutionary pathways where composition alone cannot account for the disparities in densities.

3 RESULTS: INTERNAL EVOLUTION OF OBJECTS FORMED IN THE TRANSNEPTUNIAN REGION

We model porosity evolution and the possible occurrence of aqueous alteration in several examples of mid-sized bodies representing Phoebe-like bodies formed with various amounts of ^{26}Al. The approach is similar to Castillo-Rogez et al. (2007, 2012, 2017) and Marchis et al. (2014) using porosity evolution data for various icy compositions (e.g. Leliwa-Kopystynski & Kossacki 2000; Durham, McKinnon & Stern 2005) and accounting for the insulating effect (i.e. lower thermal conductivity) of porosity (Shoshany, Prialnik & Podolak 2002). We assume accretion is near instantaneous (Leliwa-Kopystynski & Kossacki 2000). It has generally been assumed that the relative fractions of ice and rock for objects formed in the solar nebula was determined by nebula temperatures and the form (reduced or oxidized) taken by carbon, with grain densities ranging from about 1.5 to 2.2 g cm^{-3} (Wong et al. 2008; Castillo-Rogez et al. 2012). We use 1.5 and 1.8 g cm^{-3} as references densities for this modelling since the resulting models yields the best fits to the observations. The corresponding mass fractions of dry rock ranges from about 53–67 per cent. We also assume a starting bulk porosity of 50 per cent in all our models. While icy bodies in the far outer Solar system contain second-phase impurities that can promote low temperature compaction creep, their abundances are not constrained. Here, we assume that relaxation is only driven by water ice. This endmember case yields a bound on the amount of compaction driven by thermal evolution. We track microporosity evolution but not macroporosity introduced by impacts or subcatastrophic collision and reaccretion that may contribute 10–15 per cent of the overall porosity. Lastly, we account for the impact of aqueous alteration on material thermophysical properties, following the approach presented in Castillo-Rogez et al. (2019).

Results are presented in Fig. 2. Short-lived radioisotopes represent a powerful heat source that can drive long-term geophysical evolution. Times of formation of 3 and 3.5 My after CAIs allows early ice melting, aqueous alteration, and separation of an ice rich shell (Figs 2a and b). In these examples, compaction and most of the thermal evolution occurs during the first 10s of My after formation and the body freezes by 100 My. The impact of long-lived radioisotopes is negligible because of the high thermal conductivity of ice at 30 K ($\sim$16 W m^{-1} K^{-1}; Andersson & Inaba 2005).

The most recent estimate for the lifetime of the solar nebula based on magnetic measurements of meteorites is about 4 My (Wang et al. 2017). Weaker ^{26}Al decay heat resulting from later times of formation leads to partial compaction for 4 My after CAIs (Fig. 2c) or insignificant compaction if the time of formation is longer than $\sim$4.5 My after CAIs (Figs 2e and f). Hence, just 1 My delay in the formation of a Phoebe-like body leads to a very different outcome. If Phoebe-sized TNOs accreted after 4 My, then a slightly lower density (e.g. 1500 kg m^{-3}, Fig. 2d), greater initial porosity, and/or significant macroporosity are needed to reproduce a density of $<$ 1 g cm^{-3} generally observed in that group of bodies (Fig. 1). Another example, for a body 250 km in radius also suggests a grain density lower than that required for Phoebe (Fig. 3). A density of 1500 kg m^{-3} yields a bulk density of $\sim$1300 kg m^{-3}, which appears consistent with observations (noting the small sample) (Fig. 3b).

For TNOs greater than 250 km in radius, the linear trend in the density versus size seen in Fig. 1 can be ascribed to the combined effect of size and long-lived radioisotope decay heat (Brierson and Nimmo 2019). Macroporosity could shift the bulk density towards lower values, while material loss from impacts at differentiated bodies and redistribution of volatiles upon heating could increase it (Barr & Schwamb 2016). A more detailed study is required to narrow down the original grain density of KBOs.

In summary, the preservation of $>$50 per cent porosity in certain classes of small bodies can be directly ascribed to a scarcity in short-lived radioisotopes. The contrast in formation temperatures between these reservoirs is not sufficient to explain the difference in evolution. These results suggest that interior evolution of mid-sized KBOs was more limited than previously anticipated (e.g. Merk & Prialnik 2006). Similar evolution between Trojan asteroids, P- and D-type asteroids found in the main belt, Centaurs, and KBOs support a genetic relationship between these classes of bodies, as simulated by many studies (Morbidelli et al. 2005; Wong & Brown 2015; Levison et al. 2009; Vernazza et al. 2015; Vernazza & Beck 2017). This also suggests that P- and D-type asteroids found throughout the Solar system were barely chemically evolved and offer truly pristine material to sample below their weathered crust.

4 DISCUSSION AND CONCLUSIONS

Phoebe was suggested to come from the Kuiper Belt based on the observation that its density matches the grain density inferred from cosmochemical models (Johnson & Lunine 2005; Castillo-Rogez et al. 2012). The density contrast between Phoebe and KBO questions that relationship. Thermal modelling confirms earlier work showing that most of Phoebe's original porosity could be removed provided that it accreted in $\sim$3–3.5 My after calcium-aluminium inclusions (Castillo-Rogez et al. 2012). Furthermore, Phoebe displays hydrated material on its surface, which is consistent

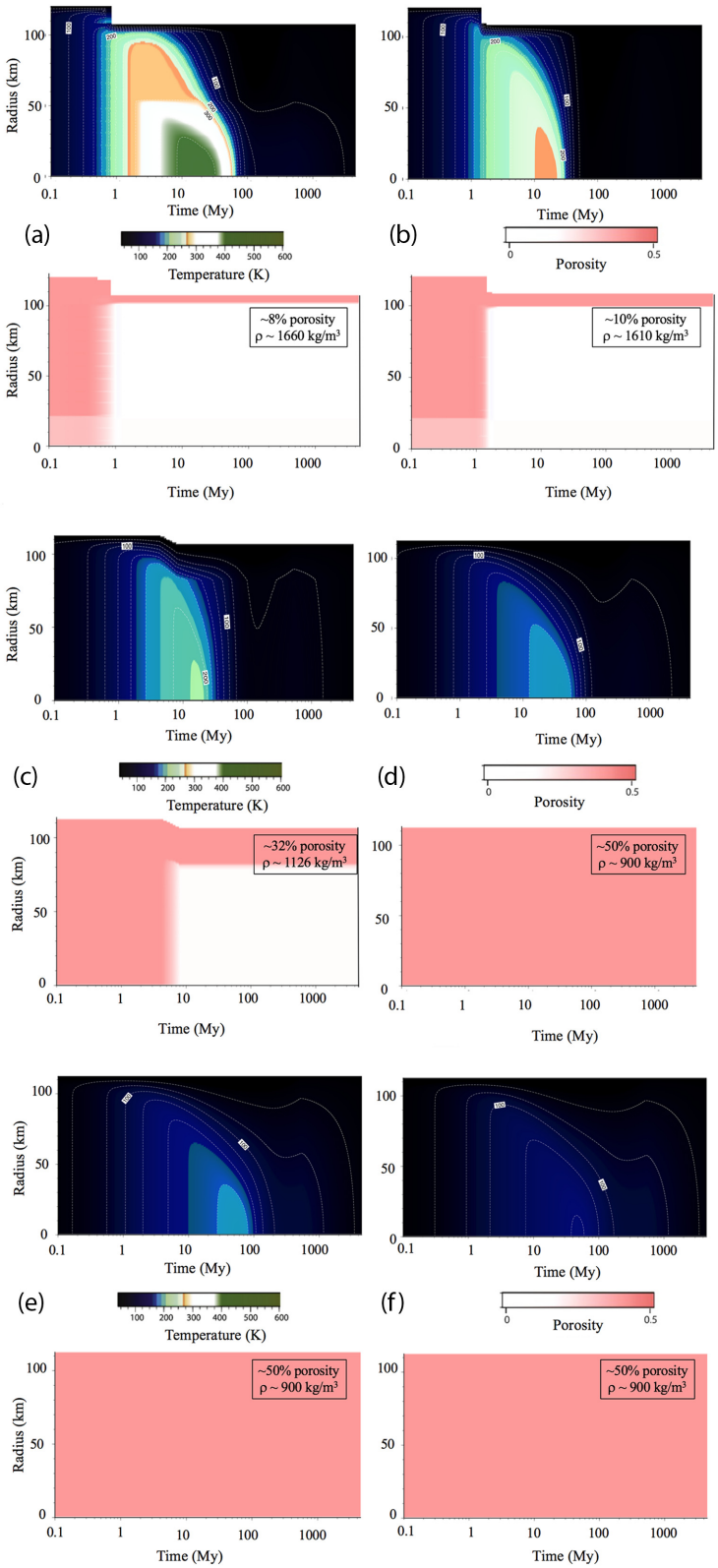

Figure 2. (a, b) Thermal and porosity evolution of Phoebe (∼107 km radius) assuming a time of formation of (a) 3 My and (b) 3.5 My after CAIs, a grain density of 1.8 g cm^{-3}, an initial bulk porosity of 50 per cent, and a formation temperature of 30 K. The final porosity and bulk density are indicated in the insets. In these two cases, the final bulk density is close to the observed density of 1.63 g cm^{-3}. (c, d) Same as 2a but assuming a Phoebe-like body formed in the transneptunian region, a time of formation of 4 My after CAIs, and a gain density of (c) 1800 kg m^{-3} and (d) 1500 kg m^{-3}. (e, f) Same as 2a (grain density of 1800 kg m^{-3}) for times of formation of (e) 4.5 My and (f) 5 My after CAIs.

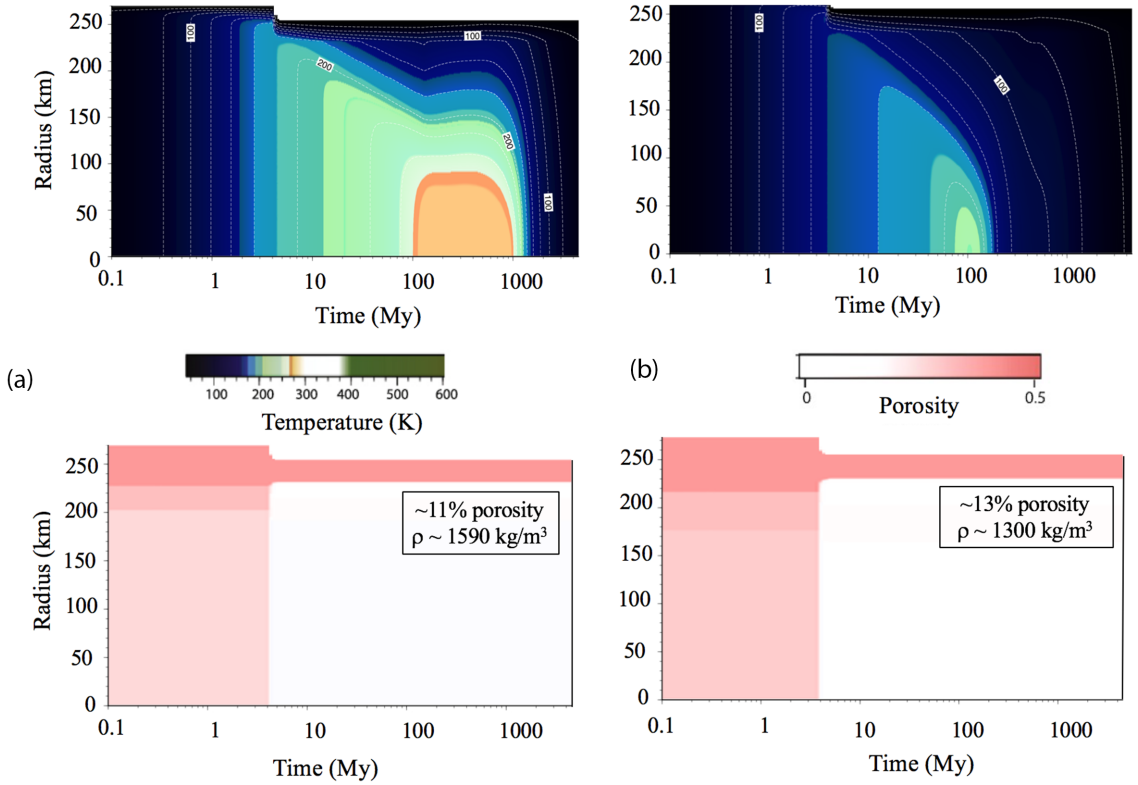

Figure 3. Same as Fig. 2, but for a 250-km radius object, a time of formation of 4 My after CAIs, and a grain density of (a) 1800 kg m^{-3} and (b) 1500 kg m^{-3}.

with internal evolution involving aqueous alteration simulated for times of formation of 3–3.5 My after CAIs (Figs 2a and b). Himalia and most of its family members display a flat spectrum in the 0.4–0.9 μm range and similar spectral properties in the visible and near infra-red as certain C-type asteroids, for example 52 Europa (Brown & Rhoden 2014; Bhatt et al. 2017). Phoebe and Himalia contrast with other irregular satellites showing a reddening that might link them to the classes of P and D asteroids (e.g. Themisto and Ananke). The latter have been interpreted as evidence for an origin of irregular satellites from a reservoir shared with KBOs. On the other hand, the similarities between the spectra of Phoebe, Himalia, and C-type asteroids was interpreted as evidence that the two irregular satellites actually migrated from the main belt of asteroids (e.g. Hartmann 1987). As an alternative, early giant planet migration and/or planetary growth (Walsh et al. 2011; Raymond and Izidoro 2017; Ronnet et al. 2018) could provide a scenario for a common origin for hydrated C-type asteroids and some irregular satellites from between the orbits of the giant planets. This model implies accretion was early and fast in that region, consistent with recent accretion scenarios (e.g. Johansen et al. 2015). As a corollary, this model suggests bodies in the Jupiter–Uranus region formed fast enough for ^{26}Al to play a role in their geophysical evolution, as suggested for Iapetus (Castillo-Rogez et al. 2007). On the other hand, short-period comets, if they are connected to the Kuiper Belt, also formed with little or no ^{26}Al, contrary to previous assumptions (e.g. Gounelle et al. 2008). The long required time of formation for TNOs, potentially longer than 4 My, needs to be reconciled with the current estimate for the solar nebula lifetime (Wang et al. 2017). Certain processes, such as the latent heat of supervolatile ice vaporization, also need to be accounted for in order to derive a most accurate timeline of events in the outer Solar system.

New main belt asteroid densities are necessary to assess whether the scattering observed across that class of bodies in Fig. 1 is real and can potentially reflect different origins across the Solar system for the various types of C-type asteroids. Density constraints will become available from observations with the Very Large Telescope at mid-sized main belt asteroids in the 2019–2020 timeframe (HARISSA Project, Vernazza et al. 2018) and by the Lucy mission at the Jupiter Trojans.

Lastly, Phoebe's evolved interior needs to be reconciled with the very high D/H ratio (0.0013 ± 0.0003) recently inferred from the infrared observations returned by the Cassini mission (Clark et al. 2019). This high value is an order of magnitude higher than that of Jupiter-Family-Comets, implying a colder accretional environment, and its meaning remains to be further understood, especially if Phoebe is not a pristine object.

ACKNOWLEDGEMENTS

The authors are grateful to Sean Raymond for his comments, which significantly improved the quality of this manuscript. JCCR is thankful to Hap McSween, Driss Takir, and Orkan Umurhan for feedback. Part of this work was carried out at the Jet Propulsion Laboratory, California Institute of Technology, under contract to NASA. Government sponsorship acknowledged.

REFERENCES

Andersson O., Inaba A., 2005, PCCP, 7, 1441
Baer J., Chesley S. R., Matson R. D., 2011, AJ, 141, 12
Baer J., Chesley S. R., 2008, Celestial Mech. Dyn. Astr., 100, 27
Barr A. C., Schwamb M. E., 2016, MNRAS, 460, 1542

Bhatt M., Reddy V., Schindler K., Cloutis E., Bhardwaj A., Corre L. L., Mann P., 2017, A&A, 608, A67
Bottke W., Jr., Durda D. D., Nesvorny D., Jedicke R., Morbidelli A., Vokrouhlicky D., Levison H., 2005, Icarus, 175, 111
Brierson C., Nimmo F., 2019, Icarus, 326, 10
Brown M. E., 2013, ApJ, 778, L34
Brown M. E., Rhoden A. R., 2014, ApJ, 793, L44
Brozovic M., Jacobson R., 2017, AJ, 153, 147
Carry B., 2012, PSS, 73, 98
Castillo-Rogez J., Matson D. L., Sotin C., Johnson T. V., Lunine J. I., Thomas P. C., 2007, Icarus, 190, 179
Castillo-Rogez J., Johnson T., Thomas P., Choukroun M., Matson D., Lunine J., 2012, Icarus, 219, 86
Castillo-Rogez J. C., Walsh K. J., Vernazza P., Takir D., 2017, Building New Worlds, 2043, 2025
Castillo-Rogez J. C., Hesse M. A., Formisano M., Sizemore H., Bland M., Ermakov A. I., Fu R. R., 2019, GRL, 46, 1963
Clark R. N. et al., 2005, Nature, 435, 66
Clark R. N., Brown R. H., Cruikshank D. P., Swayze G., 2019, Icarus, 321, 791
Consolmagno G., Britt D., Macke R., 2008, Chemie der Erde – Geochem., 68, 1
Cruikshank D. P., 1977, Icarus, 30, 224
Cuzzi J. N., Hogan R. C., Bottke W. B., 2010, Icarus, 208, 518
Delsanti A., Merlin F., Guilbert-Lepoutre A., Bauer J., Yang B., Meech K. J., 2010, A&A, 520, A40
Dermott S. F., Christou A. A., Li D., Kehoe T. J. J., Robinson J. M., 2018, Nature Astron., 2, 549
De Sanctis M. C. et al., 2015, Nature, 528, 241
Descamps P., 2015, Icarus, 245, 64
Durham W. B., McKinnon W. B., Stern L. A., 2005, Geophys. Res. Lett., 32, L18202
Fornasier S., Lantz C., Barucci M. A., Lazzarin M., 2014, Icarus, 233, 163
Fraser W. C., Brown M. E., 2018, AJ, 156, 13
Goffin E., 2014, A&A, 565, A56
Gounelle M., Morbidelli A., Bland P. A., Spurny P., Young E. D., Sephton M., 2008, in Barucci M. A., Boehnhardt H., Cruikshank D. P., Morbidelli A., eds, The Solar System Beyond Neptune. University of Arizona Press, Tucson, p. 525
Grundy W. M., et al., 2012, Icarus, 220, 74
Hartmann W. K., 1987, Icarus, 71, 57
Hanuš J., Marchis F., Viikinkoski M., Yang B., Kaasalainen M., 2017a, A&A, 599, A36
Hanuš J. et al., 2017b, A&A, 601, 41
Johansen A., Mac Low M.-M., Lacerda P., Bizzarro M., 2015, Sci. Adv., 1, e1500109
Jogo K., Nakamura T., Ito M., Wakita S., Zolotov M. Y., Messenger S. R., 2017, Geochim. Cosmoch. Acta, 199, 58
Johnson T. V., Lunine J. I., 2005, Nature, 435, 69
Leliwa-Kopystynski J., Kossacki K. J., 2000, Planet. Space Sci., 48, 727
Levison H. F., Bottke W. F., Gounelle M., Morbidelli A., Nesvorný D., Tsiganis K., 2009, Nature, 460, 364
Licandro J., Campins H., Kelley M., Hargrove K., Pinilla-Alonso N., Cruikshank D., Rivkin A. S., Emery J., 2011, A&A, 525, A34
Marchis F., Kaasalainen M., Hom E. F. Y., Berthier J., Enriquez J., Hestroffer D., Le Mignant D., de Pater I., 2006, Icarus, 185, 39
Marchis F., Descamps M., Baek M., Harris A. W., Kaasalainen M., Berthier J., Hestroffer D., Vachier F., 2008, Icarus, 196, 97
Marchis F. E. et al., 2012, Icarus, 221, 1130
Marchis F. et al., 2013, Icarus, 224, 178
Marchis F. et al., 2014, ApJ, 783, L37
McAdam M. M., Sunshine J. M., Howard K. T., McCoy T. J., 2015, Icarus, 245, 320
Meech K. J., Buie M. W., Samarasinha N. H., Mueller B. E. A., Belton M. J. S., 1997, AJ, 113, 844
Merk R., Prialnik D., 2006, Icarus, 183, 283
Morbidelli A., Levison H. F., Tsiganis K., Gomes R., 2005, Nature, 435, 462
Morbidelli A., Bottke W. F., Nesvorny D., Levison H. F., 2009, Icarus, 204, 558
Müller T. G., et al., 2009, Earth, Moon, and Planets, 105, 209
Pajuelo M. et al., 2018, Icarus, 309, 134
Porco C. C. et al., 2003, Science, 299, 1541
Prialnik D., Sarid G., Rosenberg E. D., Merk R., 2008, Space Sci. Rev., 138, 147
Raymond S. N., Izidoro A., 2017, Icarus, 297, 134
Rivkin A. S., Thomas C. A., Howell E. S., Emery J. P., 2015, AJ, 150, 198
Ronnet T., Mousis O., Vernazza P., Lunine J., Crida A., 2018, AJ, 155
Schramm D. N., Tera F., Wasserburg G. J., 1970, Earth Planet. Sci. Lett., 10, 44
Shschuko O. B., Shschuko S. D., Kartashov D. V., Orosei R., 2014, Planet. Space Sci., 104, 147
Shoshany Y., Prialnik D., Podolak M., 2002, Icarus, 157, 219
Somenzi L., Fienga A., Laskar J., Kuchynka P., 2011, PSS, 58, 858
Stansberry J. A. et al., 2012, Icarus, 219, 676
Tegler S. C., Romanishin W., Consolmagno G. J., Rall J., Worhatch R., Nelson M., Weidenschilling S., 2005, Icarus, 175, 390
Thomas P. C. et al., 2007, Icarus, 190, 573
Vernazza P. et al., 2015, ApJ, 806, 10
Vernazza P. et al., 2016, AJ, 152, 54
Vernazza P. et al., 2017, AJ, 153, 10
Vernazza P., Beck P., 2017, in Elkins-Tanton L. T., Weiss B. P., eds, Planetesimals: Early Differentiation and Consequences for Planets. Cambridge Univ. Press, Cambridge
Vernazza P. et al., 2018, A&A, 618, 16
Vilenius E. et al., 2012, A&A, 541, 17
Walsh K. J., Morbidelli A., Raymond S. N., O'Brien D. P., Mandell A. M., 2011, Nature, 475, 206
Wang H. et al., 2017, Science, 355, 623
Wong M. H., Lunine J. I., Atreya S. K., Johnson T. V. , Mahaffy P. R., Owen T. C., Encrenaz T., 2008, in MacPherson G. J., ed., Reviews in Mineralogy and Geochemistry, vol. 68. Mineralogical Society of America. Chantilly, VA, p. 241
Wong I., Brown M. E., 2015, AJ, 150, 174
Yeomans D. K. et al., 1997, Science, 278, 2106
Young E. D., Ash R. D., England P., Rumble D., III, 1999, Science, 286, 1331
Young E. D., Zhang K. K., Schubert G., 2003, Earth Planet. Sci. Lett., 213, 249

This paper has been typeset from a Microsoft Word file prepared by the author.